RAISER Conference 2021

International Conference on Recent Advances in Sustainable Energy Research 2021 (RAISER 2021)
July 6-7, 2021
Penang, Malaysia

Flow and Heat Transfer Simulation Analysis of 3D Compact Heat Exchanger

G. Sashwin Nair [1,*], A. N. Oumer[1], Azizuddin Abd Aziz[2], J. P. Siregar[1]

[1] Department of Mechanical Engineering, College of Engineering, University Malaysia Pahang, Pahang, Malaysia
[2] Faculty of Mechanical and Automotive Engineering Technology, University Malaysia Pahang, Pahang, Malaysia

ARTICLE INFO

Article history:
Received xxxxxxx
Received in revised form xxxxxxx
Accepted xxxxxxx
Available online xxxxxxx

Keywords:
Numerical simulation; Compact heat exchangers; laminar flow; heat transfer; pressure drop

ABSTRACT

One of the most common heat exchangers (HEs) utilized in the industry is a compact heat exchanger due to its superior advantage over other types of heat exchangers. Various geometric (fin spacing, tube inclination angle, etc) and process (such as flow velocity, temperature, etc) parameters affect the performance of such compact HEs. The objective of this paper is to investigate the effects of fin spacing, tube inclination angle, and airflow velocity for both tube configurations which are inline and staggered arrangements on heat transfer and pressure drop performance of fin-and-tube HEs. A three-dimensional (3D) numerical method with the aid of Ansys FLUENT software was carried out for the laminar flow condition. Based on the obtained results, the highest average heat transfer coefficient was observed at 120° for both tube arrangements while the lowest average pressure drop penalty is at 30°. Therefore, the recommended inclination angle when high heat transfer is needed is at 120° while if the pumping power is the major problem, 30 °or 150° is recommended.

1. Introduction

In this generation, there are various types of heat exchanger (HE) used in industry and it's selected based on their applications. The most familiar HEs utilized in the industry are shell and tube HE, plate HE, fin-and-tube HE, condensers, boilers and evaporators. For this study, the compact heat exchanger (CHE) was chosen due to its light weight, small size and cheap. Examples of CHEs that are usually used are plate HE, fin-and-tube HE and spiral HE [1]. In this study, fin-and-tube was selected due to its superior advantage over other types of HE. This HE is commonly used to enhance the heat transfer performance due to its larger heat transfer surface area per volume and is regularly used in car radiators which the flow in this type of HE is usually in the laminar range [2]. Recently, there is various research regarding the geometric and process parameters effect on the heat transfer performance of CHE [3-8]. Moreover, the pressure drop has been given attention to the HE performance as higher pressure requires higher cost. Thus, the most challenging part for the researchers is to improve the HE's geometry to ensure enhanced heat transfer across the HE together with low pressure drop.

Firstly, the flat tube's thermal-hydraulic diameter is smaller than a circular tube. Utilizing circular tubes in HE has several disadvantages such as high drag induced on the tube and low heat transfer on the fin behind the tube. This is due to behind the tubes, a low-velocity wake region is formed. These disadvantages can be solved by using oval or flat tubes in HE. Apart from that, it is proven that

flat-tube HE gives a higher air-side heat transfer coefficient with a low-pressure drop. [9]. Several process and geometric parameters affect the performance of heat transfer on CHE including the shape of tube and fin, fin pitch, tube pitch, tube arrangement and tube angle. Various experimental and numerical research has been done to investigate the air-side heat and flow performance using different fin shapes. H. Ke et al. [10] reported that a wavy fin gives a higher Nusselt number than a plain fin due to the interruption of the flow which creates a twisting flow at the wake of the tube. Apart from that, Duan et.al [11] proven that by using a wavy fin with a flat tube, longitudinal and transverse vortices are formed which improves the heat transfer. Furthermore, S. Sakib and A. Al-Faruk [12] stated that the higher surface area of heat transfer of rectangular fin causes the heat transfer of the fin to be enhanced. M.Zeeshan et al. [13] numerically performed an investigation with inline and staggered tube arrangement to analyze the heat transfer performance of CHE. They found that staggered arrangement shows a higher heat transfer characteristic than inline arrangement as the vortex formation is seen in each row which plays the major role in heat transfer enhancement. Besides that, the most recent research by S.Unger et al. [14] states that staggered arrangement gives 88.55 % higher heat transfer enhancement than inline arrangement as the flow being deflected which improve the thermal mixing. S.Toolthaisong and N.Kasayapanand [15] had experimentally investigated the tube inclination angle of CHE on the heat transfer performance. Based on their results, the minimum and maximum heat transfer is at 0° and 90°. P.Wang et al. [3] results show that when the tube is rotated at 30°, the heat transfer coefficient is highest. Many types of research work on tube arrangement on heat transfer performance were done by many researchers. [7, 8, 16, 17]. Moreover, many research works have been done on the effect of various tube angles on the heat transfer performance of CHE. [3, 4, 15, 18]. The study related to the tube arrangement and tube angle has been done separately. However, the combination of both studies is something new and has not been fully analyzed in comparison with plain fin for an enhanced heat transfer performance.

The purpose of this study is to investigate the effect of tube inclination angle with inline and staggered tube arrangement of fin-and-tube HE on the heat transfer performance. A numerical method formulated on ANSYS FLUENT software was investigated with seven tube inclination angles. (0°, 30°, 60°, 90°, 120°, 150°) in low Reynold's number. The laminar model was utilized since the maximum inlet velocity was set at a low value. This study would help engineers to decide the angle of inclination and design the CHE for an improved heat transfer performance with low pressure drop. Moreover, engineers that are designing a high energy efficiency CHE might also be helpful from this study.

2. Methodology

2.1 Method and Materials

The schematic diagram of fin and tube cross-sections used in this study are shown in Figure 1. Tube arrangements considered in this study are in-line and staggered configurations. Air flowed across the surface of the fin and tubes and constant heat flux was contributed from the surfaces of the inner tube. The HE's model consists of an overall length of the flat tube of 220 mm and 15.1 mm tube hydraulic diameter. Square-shaped fins were used with the dimension of 110 mm x 110mm and 0.6 mm thickness while Table 1 shows the other geometric parameters of the HE whereas Table 2 shows the properties of air. In this study, the geometric parameters of the HE are considered as previous work done by A.Y.Adam et.al. [18].

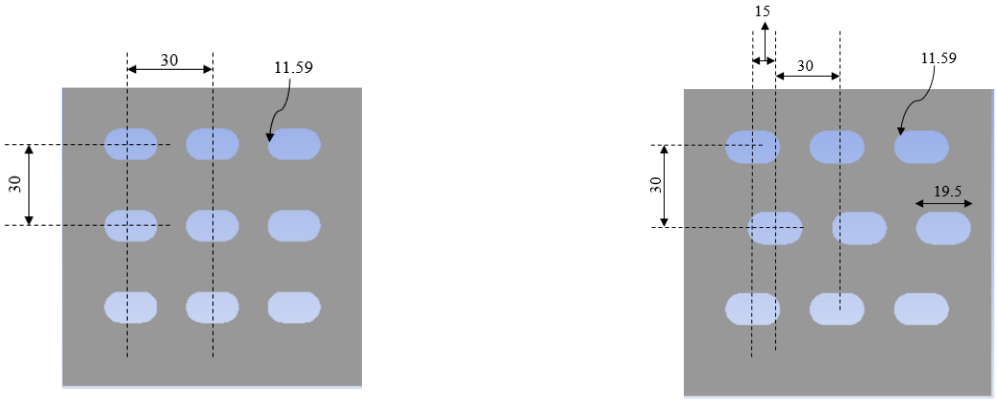

(a) (b)

Fig. 1. Schematic diagrams of the cross-section of HE with a) in-line and b) staggered arrangement. (Dimensions in mm)

Table 1
Geometric Parameters of HE

Name	Value (mm)	Symbol
Transverse pitch	30	P_t
Longitudinal pitch	30	P_l
Outside diameter of tube	11.59	D_o
Hydraulic diameter of tube	15.1	D_h
Thickness of fin	0.6	t
Spacing of fin	20	F_s
Material of tube and fin	-	Al

Table 2
Properties of Air

Name	Value	Symbol
Density	1.225 kg/m^3	ρ
Specific heat	1006.43 J/kg.K	c_p
Thermal conductivity	0.0242 W/m.K	k
Viscosity	1.7894 x 10^{-5} kg/m.s	μ

2.2 Computational Domain

The computational domain of 3 rows by 3 columns for both tube configurations is shown in Figure 2. At the upstream, the computational domain was extended 2 times the tube outer diameter (D_o) to form a fully developed constant velocity flow. Besides, the domain was extended 5 times the tube outer diameter to avoid airflow recirculation and to make sure the boundary layer formation at the outlet is fully developed. [8]. A 2D view of the inlet and outlet extension with boundary conditions is shown in Figure 3. Symmetry conditions were used in right, left, top and bottom of the test section.

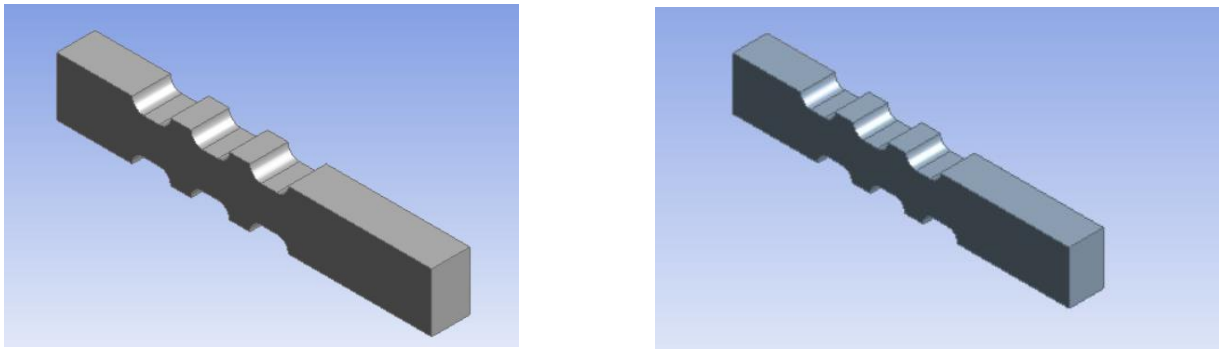

(a) (b)

Fig. 2. Computational domain of a) in-line and b) staggered arrangement

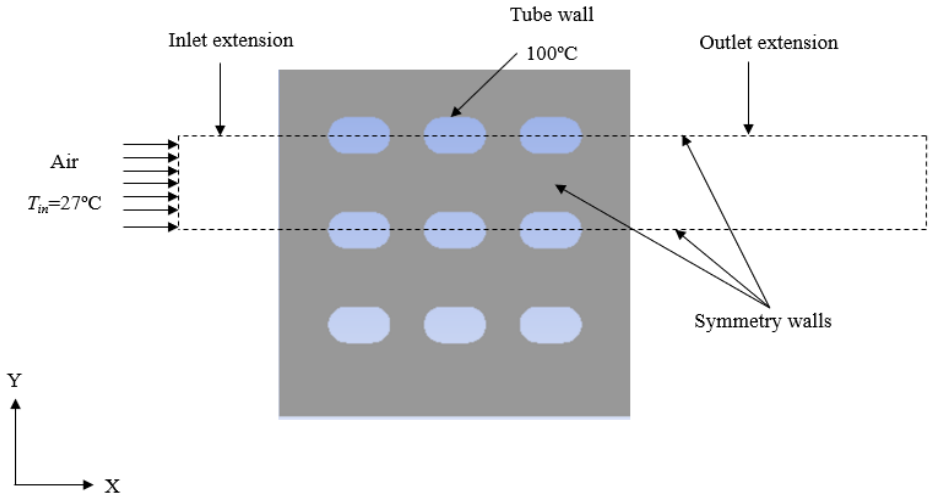

(a)

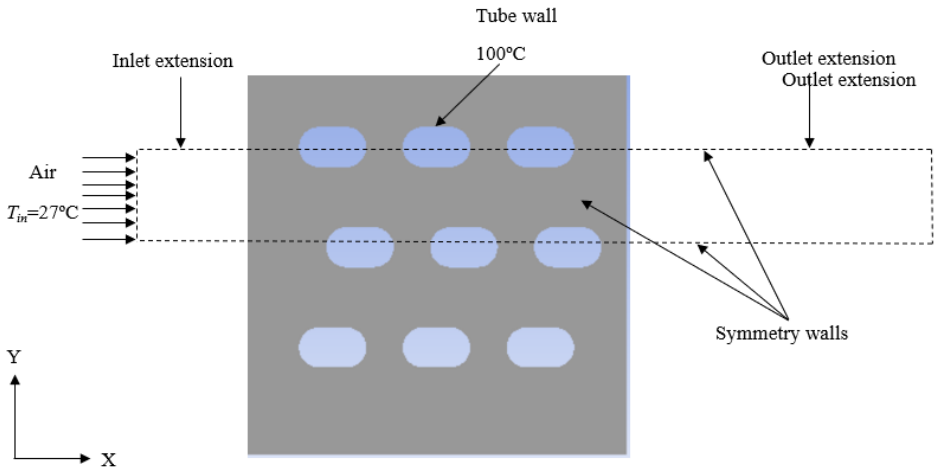

(b)

Fig. 3. 2D view of computational domain with boundary conditions for a) in-line and b) staggered arrangement.

2.3 Mathematical Equation
2.3.1 Governing Equation

The numerical formulation is based on the assumption of an incompressible, turbulent, non-isothermal and consistent stream region. Furthermore, the physical properties are considered to be constant, thermal radiation and heat dissipation are not taken into consideration, and the fin surfaces are assumed to be smooth. The continuity, momentum and energy governing equations, as well as the transport equation of turbulent kinetic energy and its dissipation rate, are all described based on these assumptions. The equations for continuity, momentum and energy will be as follows:

$$\nabla.(V) = 0 \quad (1)$$

$$\rho\nabla.(\boldsymbol{VV}) = -\nabla P + \nabla.\tau \quad (2)$$

$$\rho C p\nabla.(T\boldsymbol{V}) = k\nabla.T \quad (3)$$

2.3.2 Parameters Definitions

The airflow and geometry of the HE determine heat transfer and pressure drop characteristics for compact HE. The heat transfer coefficient between the finned flat tube and air is shown in the equation below. [17]:

$$h = \frac{\dot{Q}}{A(T_s - T_b)} \quad (4)$$

$$T_b = \frac{T_{in} + T_{out}}{2} \quad (5)$$

where $\dot{Q}$ is the heat transfer rate, A is the total surface area including fins and tubes, T_s is the tube wall surface temperature and T_b is bulk fluid temperature.

The pressure drop is the difference between the outlet and inlet pressure of the flow, written as [7]:

$$\Delta P = P_{in} - P_{out} \quad (6)$$

The boundary conditions used in the computations are shown as follows:

i. A uniform velocity and temperature (300 K) are fixed at the inlet boundary.
ii. All tube walls have no-slip conditions. The test section's lateral surfaces are given symmetry conditions.
iii. The temperature of the tube walls is set to 373 K.
iv. The computational domain is expanded downstream for a fully developed outlet boundary state.
v. Other surfaces are assigned symmetrical boundary conditions.

2.4 Meshing

2.4.1 Mesh Metrics Quality

Mesh Metrics are the most practical quality to determine the accurate shape and size of the elements. Before proceeding to the mesh independency test, the mesh metrics quality needs to be in the appropriate range. In this study, orthogonal, skewness and aspect ratio were taken into consideration. The range for good mesh metrics as follows;

i. Orthogonal = min > 0.25
ii. Skewness = max < 0.8
iii. Aspect ratio = max < 40

Based on table 2, the value for each mesh metric is in the allowable range. Thus, the quality of the mesh is acceptable.

Table 2
Mesh metrics quality

Mesh	**Number of grids**	**Mesh Metrics Quality**		
		Orthogonal	**Skewness**	**Aspect Ratio**
1	55605	Min = 0.47692	Max = 0.62748	Max = 11.321
2	60660	Min = 0.47692	Max = 0.62748	Max = 11.182
3	65715	Min = 0.47692	Max = 0.62748	Max = 10.24
4	93092	Min = 0.54988	Max = 0.57556	Max = 8.0932
5	109000	Min = 0.67648	Max = 0.66875	Max = 4.0141

2.4.2 Mesh Independency Test

A mesh independency test was carried out with 5 different grid sizes which are 55605, 60660, 65715, 93092 and 109000. In this test, in-line arrangement with 1.8 m/s inlet velocity was kept constant. The mesh independency test for the five different grid sizes is shown in Figure 4. The difference in velocity between mesh 93092 and 109000 is shown to be 7.88 %, which is less than 10%. The outcome is acceptable as it saves computational time and space without compromising the simulation results. Thus, the finalize grid size used in this study is 93092.

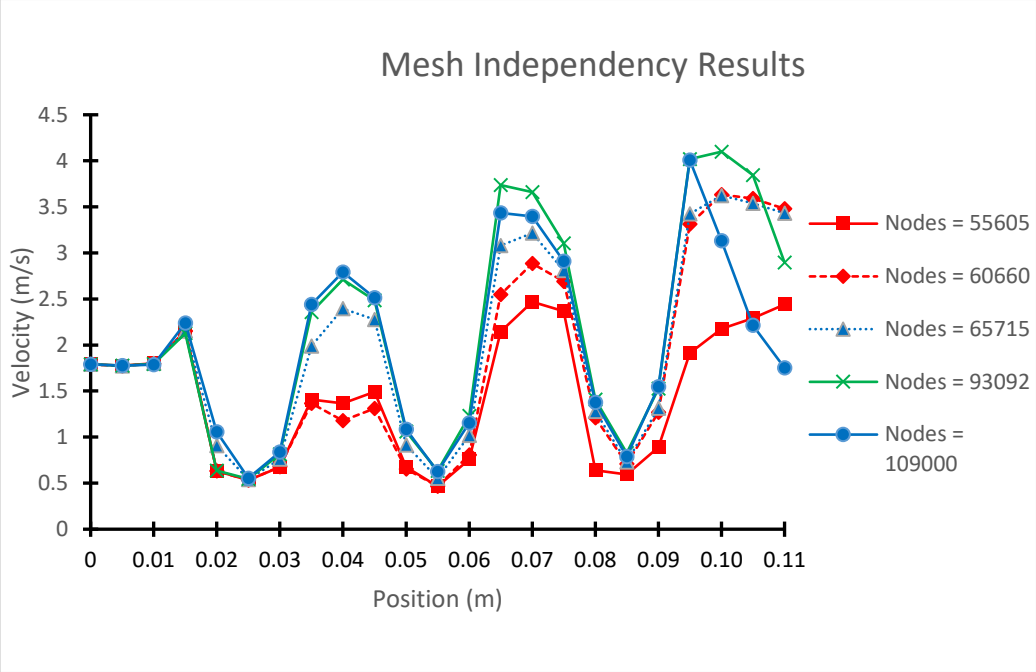

Fig. 4. Mesh independency test

2.5 Model Validation

To check the validity of the numerical model, the outlet temperature of the model was compared with the results presented by A. Y. Adam [19]. Figure 5 shows the variation of outlet temperature with inlet air velocity. The maximal deviation between the outlet temperature of the present study and experimental results was 9.8%. This clearly shows that the outlet temperature value of the present study lies within the allowable range of error as several previous research error shows more than 9.8% and they assume the model is valid. [7, 8, 18]. Therefore, good acceptance between the present study and previous research study shows that the numerical model is valid to determine the heat transfer performance and pressure drop characteristics.

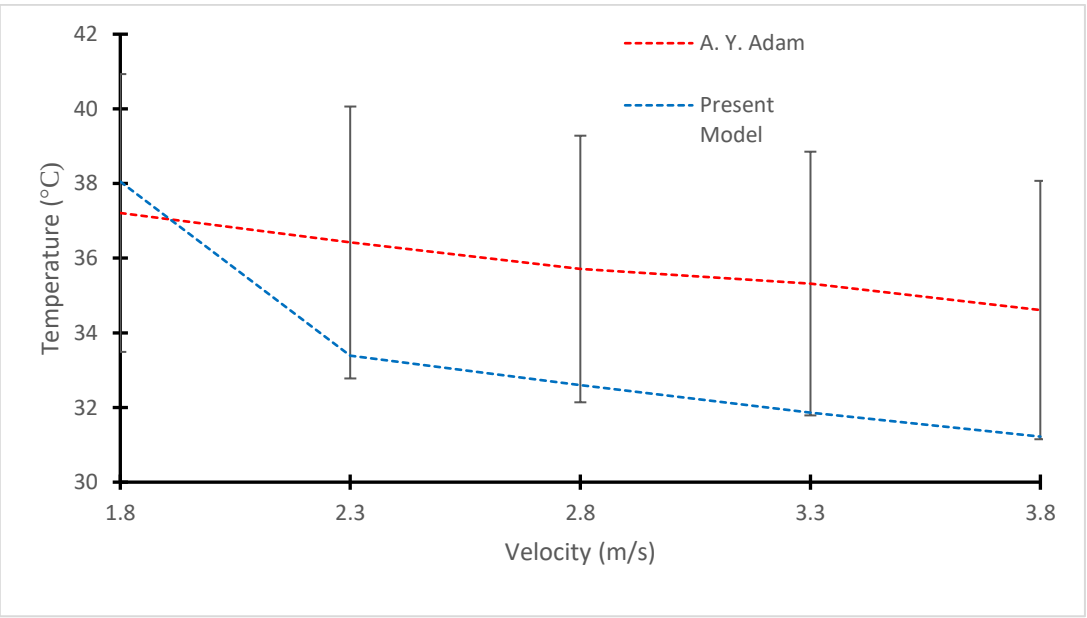

Fig. 5. Model Validation

3. Results and Discussion

3.1 Flow and Temperature Visualization

3.1.1 Flow Visualization

At an airflow velocity, v=1.8m/s, Figures 6 and 7 illustrate the effect of tube inclination angle on the flow distribution for both inline and staggered tube arrangements. Based on the results, it is obvious that recirculation occurs after each tube for both inline and staggered tube arrangements. Due to the blockage of tube, when air flows across the fin, flow separation occurs. Except for 30°, 60°, and 90° tube inclination angles, as the flow separates at the back of the tube, it bounces back at the frontal area of the subsequent tube, resulting in a larger region. This study mainly to figure out the air-side thermal performance of the CHE rather than the fin-side. The contours displayed in Figure 6 and 7 are not the fin but the spacing between the two fins. This can be the reason why the back of the successive tube doesn't show a bigger region from the flow separation. Furthermore, the flow velocity is higher at the tube wall region which makes that region effective for the heat transfer process [20].

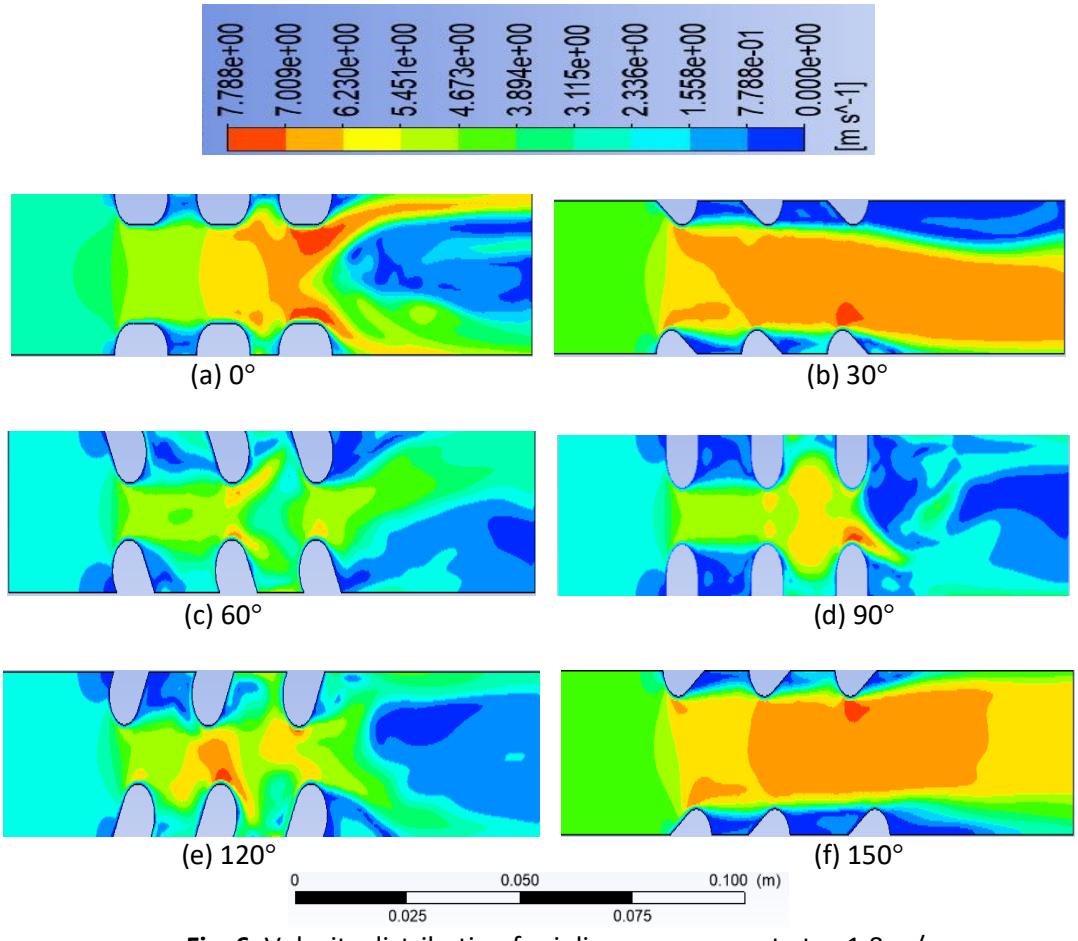

Fig. 6. Velocity distribution for inline arrangement at v=1.8 m/s

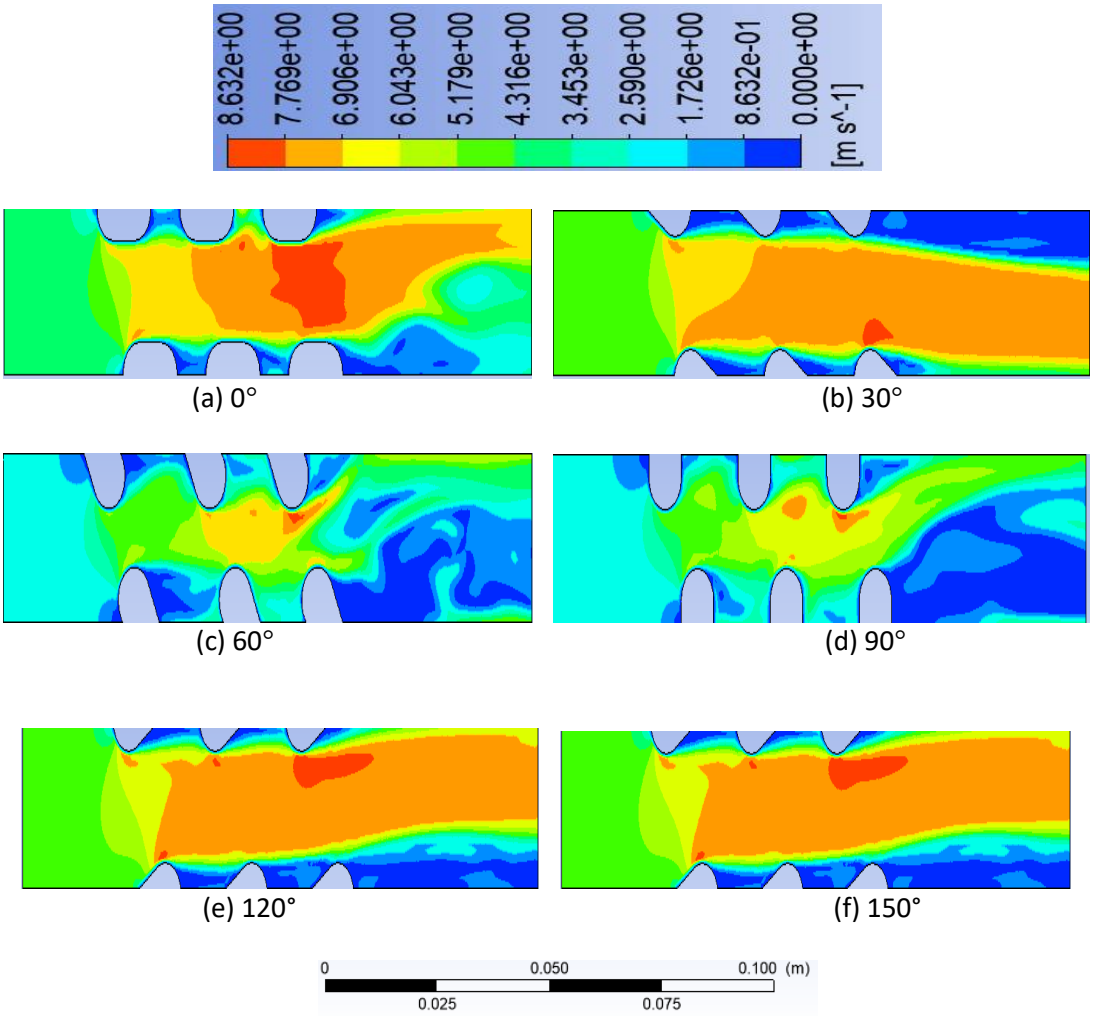

Fig. 7. Velocity distribution for staggered arrangement at v=1.8m/s

3.1.2 Temperature Visualization

At an airflow velocity, v=1.8m/s, Figures 8 and 9 display the effect of tube inclination angle on the temperature distribution for both inline and staggered tube arrangements.Based on the temperature contours below, before the flow reached the tube, the entire inlet region is at the same temperature which is at 300K. Apart from that, it is expected as the temperature is highest at the tube wall region. Based on the figures, the outlet temperature of all tube inclination angle is different. Enlarging the thermal boundary layer along the tube wall region is one of the most important factors in improving heat transfer. From 0° to 60°, the boundary layer thickness at the 3rd row of the tube is larger than the 1st row of the tube because larger air velocity around the 1st row tube before it travels to 3rd row of tube [20].

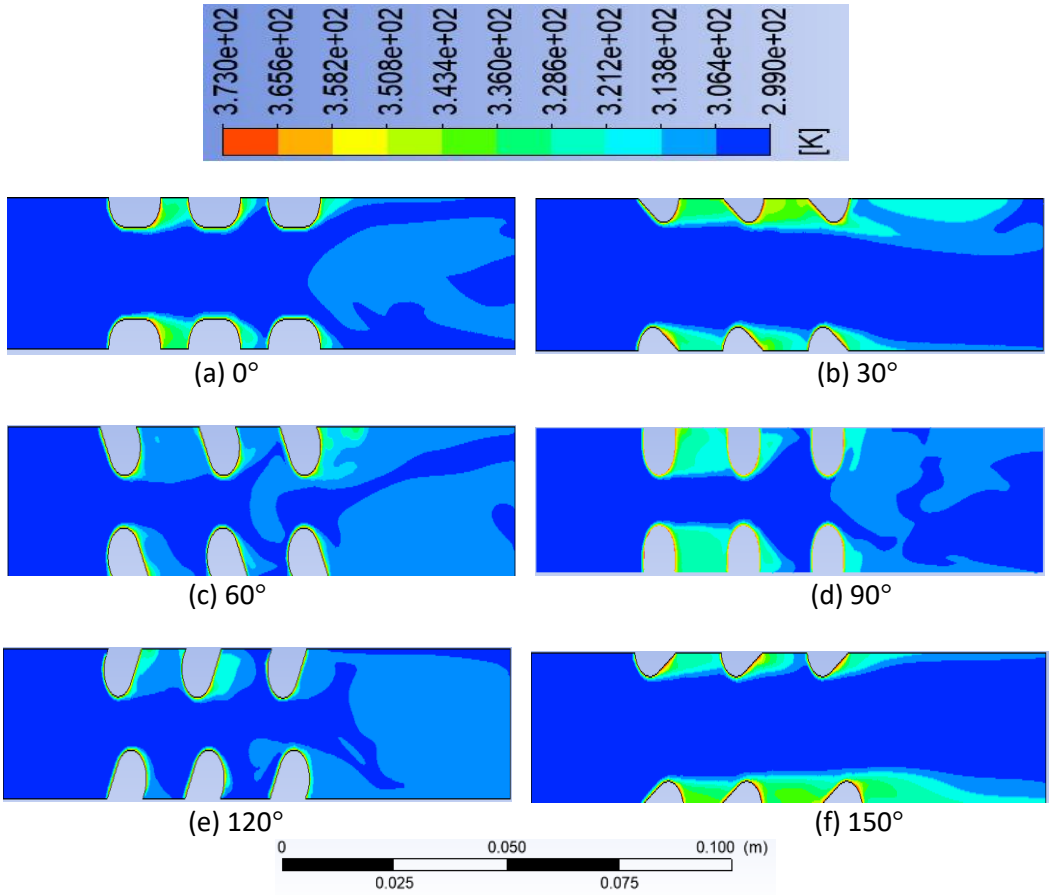

Fig. 8. Temperature distribution for inline arrangement at v=1.8 m/s

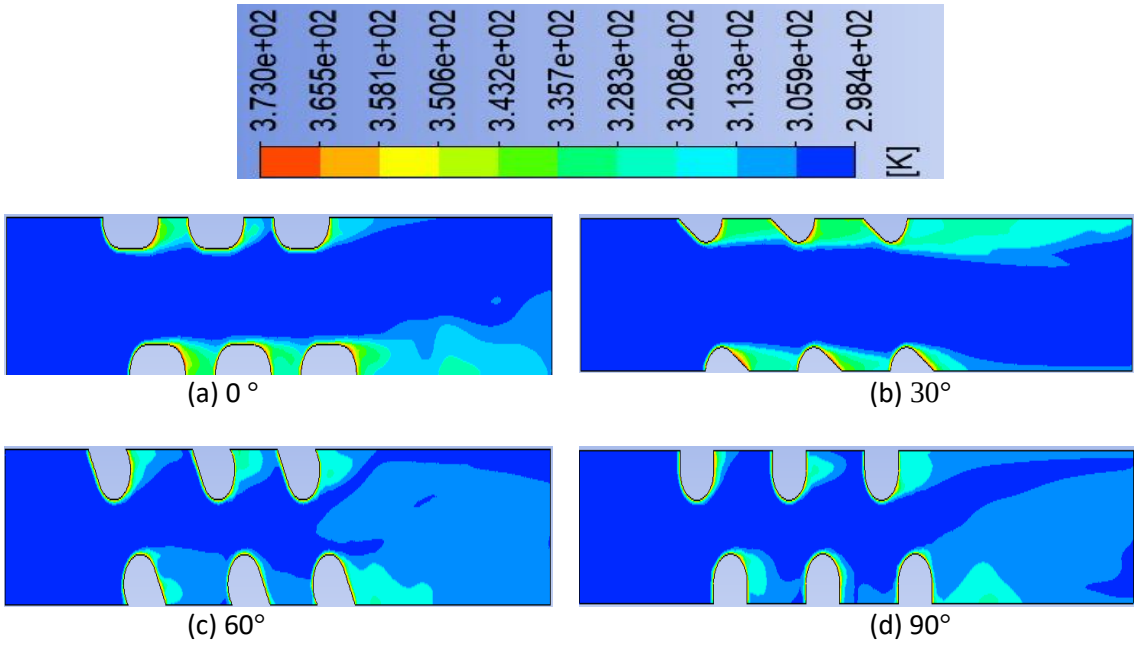

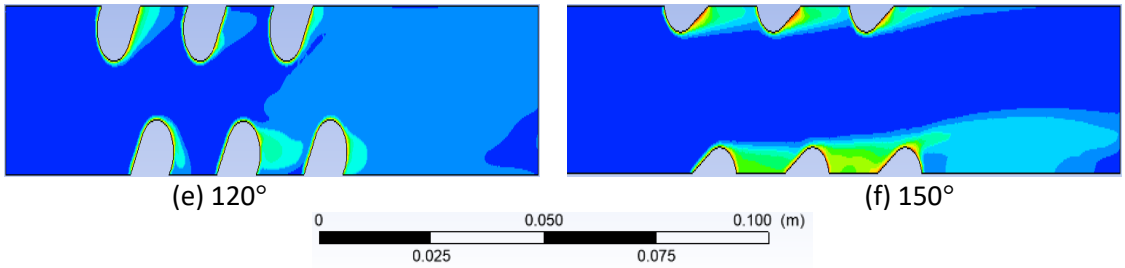

(e) 120° (f) 150°

Fig. 9. Temperature distribution for staggered arrangement at v=1.8 m/s

3.2 Flow and Heat Transfer Performance

3.2.1 Variation of h with inlet v at 0° inclination angle for inline and staggered arrangement.

Figure 10 shows the variance of heat transfer coefficient with inlet velocity for both arrangements at a 0° tube inclination angle. The heat transfer coefficient for inline arrangement increases with the inlet airflow velocity, while the heat transfer coefficient for staggered arrangement increases until 3.3 m/s and then decreases slightly until 3.8 m/s, as shown in the results. Higher velocity creates more disturbance to the thermal boundary layer which is caused by the higher strength of vortices produced from the higher velocity. In comparison with inline and staggered, inline arrangement shows a higher average heat transfer coefficient than staggered arrangement. This can be due to the tube around the staggered arrangement displays an unsymmetrical flow [18].

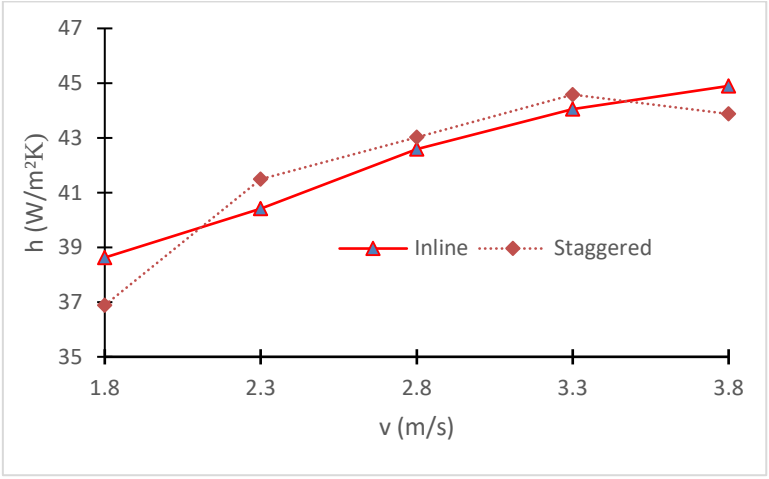

Fig. 10. Heat transfer coefficient against inlet velocity v at 0°

3.2.2 Effect of Inlet Velocity on ΔP

Figure 11 depicts the difference of pressure drop with inlet velocity for both inline and staggered arrangements at a 0° tube inclination angle. Based on Figure 11, both inline and staggered arrangement, when the inlet velocity increases, the pressure drop also increases. Hoffmann et al. stated that the static pressure changes from one tube row to another. Higher velocities passing through the fin creates a larger segment of static pressure [21]. It is clearly observed that the staggered arrangement gives a lower average pressure drop than inline arrangement. This phenomenon might be because, during the recirculation zone, two different types of forces are formed which are pressure and drag forces. This might be the reason for the pressure loss in the recirculation region.

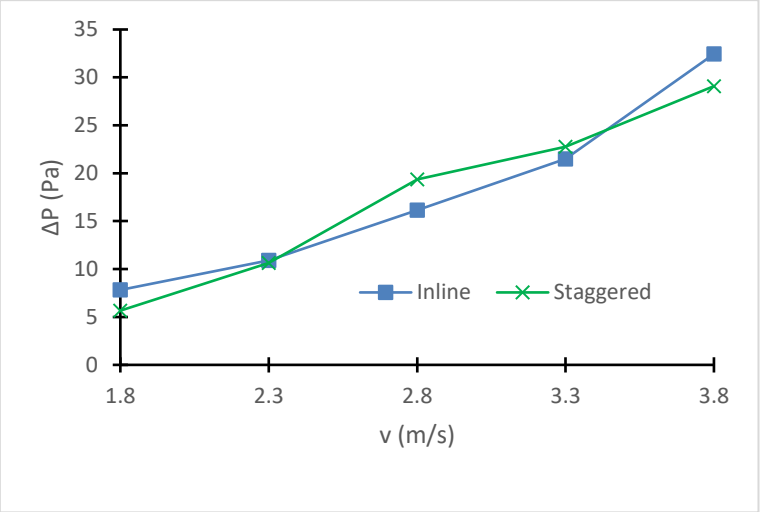

Fig. 11. Pressure drop against inlet velocity v at 0°

3.2.1 Effect of Tube Inclination Angle on h

Variations of heat transfer coefficient for inline and staggered arrangements with different tube inclinations at constant velocity of v=2.8 m/s are provided in this section. As shown in Figure 12, the heat transfer coefficients for different tube inclination angles have different values. For both inline and staggered arrangement, when the inclination is at 120°, it gives the highest heat transfer coefficient. This may be due to a delay in flow separation, resulting in a stable and consistent reduction in the wake region behind the tube. [8]. As predicted, the heat transfer coefficient value for 30° and 60° were almost the same with 150° and 120° respectively which is the same as the results claimed by Adam et al. [18]. Apart from that, the average heat transfer coefficient for inline arrangement is higher than the staggered arrangement. This phenomenon can be due to the blockage of air when it passes through the computational domain in a staggered arrangement. Therefore, less heat transferred air passes through the outlet region.

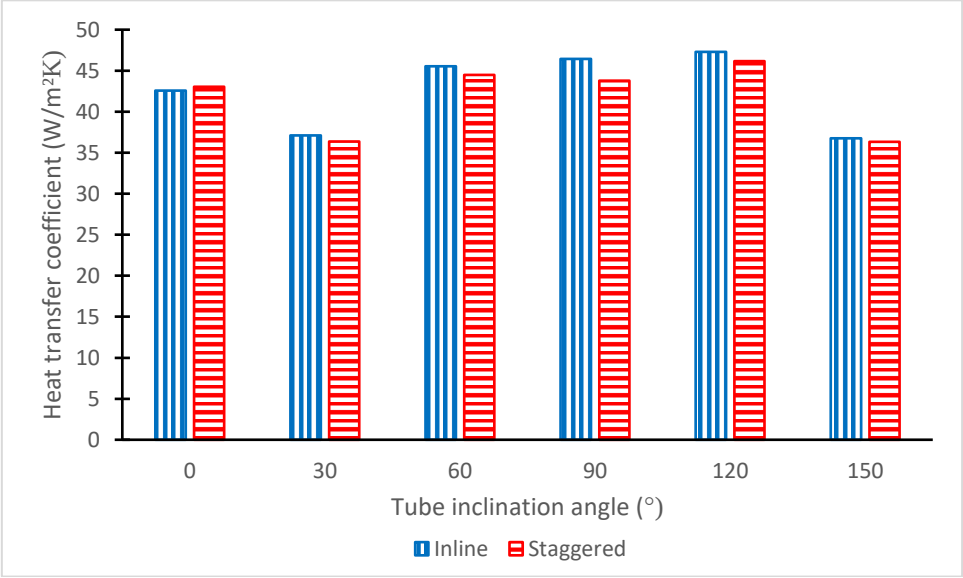

Fig. 12. Heat transfer coefficient against tube inclination angle at v=2.8 m/s

3.2.2 Effect of Tube Inclination Angle on ΔP

This section describes the variation of pressure drop with v=2.8 m/s at various tube inclination for inline and staggered arrangements. Based on Figure 13, it is obvious that the results have a different value of pressure drop for different tube inclination angles. For inline arrangement, 120° and 30° gives the highest and lowest pressure drop respectively while for staggered arrangement, 90° and 150° gives the highest and lowest pressure drop. Comparing both inline and staggered arrangement, Figure 13 shows that the average pressure drop is lower for staggered arrangement. The high value of pressure drop obtained might be because the tubes surface area intersect the air flow is large which gives extra drag and causing blockage of airflow by the tube [18]. In conclusion, by tilting the tubes at a certain angle together with a high pressure drop, heat transfer can be improved.

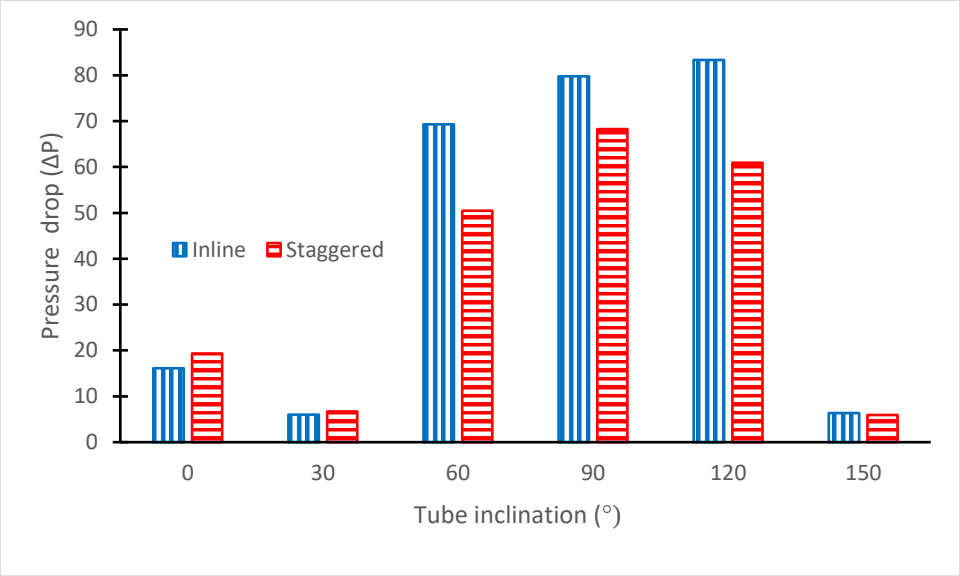

Fig. 13. Pressure drop against tube inclination angle at v=2.8 m/s

4. Conclusions

The heat transfer efficiency and pressure drop of inline and staggered tube arrangement CHE with various tube inclination angles were investigated using 3D numerical simulations in this research. The maximum and minimum heat transfer coefficients were found to be 120° and 30°, respectively, according to the numerical results. Additionally, for both configurations, the 120° tube inclination angle provides the best heat transfer and pressure drop. Thus, 120° is recommended when researchers or engineers require a high heat transfer in their work. Apart from that, if the pumping power is the main issue, 30° or 150° tube inclination is recommended. According to this study, the tube inclination angle plays a significant role in heat transfer enhancement, such as flow separation delay and reduction in the wake region behind the tube. As a final result, an enhanced heat transfer can occur. Lastly, in comparison of inline and staggered arrangement, both give almost the same heat transfer performances. Thus, for the pressure drop penalty, staggered arrangement shows a lower pressure drop than inline arrangement.

Acknowledgement
The authors are grateful to the University of Malaysia Pahang for providing the requisite support under project no. RDU 190319.

References

[1] B. Zohuri, "Heat Exchanger Types and Classifications," 2017, pp. 19-56.
[2] A. J. G. Yunus A.Cengel, *Heat and mass Transfer*, 5th ed. New York: McGraw-Hill, 2015, p. 944.
[3] P. Wang, J. Jiang, S. Li, X. Luo, S. Wang, and W. Zhao, "An investigation of influence factor including different tube bundles on inclined elliptical fin-tube heat exchanger," *International Journal of Heat and Mass Transfer,* vol. 142, p. 118448, 2019/10/01/ 2019.
[4] L. Tang, X. Du, J. Pan, and B. Sundén, "Air inlet angle influence on the air-side heat transfer and flow friction characteristics of a finned oval tube heat exchanger," *International Journal of Heat and Mass Transfer,* vol. 145, p. 118702, 2019/12/01/ 2019.
[5] H. Naik and S. Tiwari, "Thermal performance analysis of fin-tube heat exchanger with staggered tube arrangement in presence of rectangular winglet pairs," *International Journal of Thermal Sciences,* vol. 161, p. 106723, 2021/03/01/ 2021.
[6] A. Gupta, A. Roy, S. Gupta, and M. Gupta, "Numerical investigation towards implementation of punched winglet as vortex generator for performance improvement of a fin-and-tube heat exchanger," *International Journal of Heat and Mass Transfer,* vol. 149, p. 119171, 2020/03/01/ 2020.
[7] A. J. Modi, N. A. Kalel, and M. K. Rathod, "Thermal performance augmentation of fin-and-tube heat exchanger using rectangular winglet vortex generators having circular punched holes," *International Journal of Heat and Mass Transfer,* vol. 158, p. 119724, 2020/09/01/ 2020.
[8] A. J. Modi and M. K. Rathod, "Comparative study of heat transfer enhancement and pressure drop for fin-and-circular tube compact heat exchangers with sinusoidal wavy and elliptical curved rectangular winglet vortex generator," *International Journal of Heat and Mass Transfer,* vol. 141, pp. 310-326, 2019/10/01/ 2019.
[9] N.-H. Kim, S.-H. Kim, H.-W. Byun, and E.-J. Lee, "Dry and Wet Air-Side Performance of a Louver," *International Refrigeration and Air Conditioning Conference,* 2010.
[10] H. Ke *et al.*, "Thermal-hydraulic performance and optimization of attack angle of delta winglets in plain and wavy finned-tube heat exchangers," *Applied Thermal Engineering,* vol. 150, pp. 1054-1065, 2019/03/05/ 2019.
[11] F. Duan, K. Song, H. Li, L. Chang, Y. Zhang, and L. Wang, "Numerical study of laminar flow and heat transfer characteristics in the fin side of the intermittent wavy finned flat tube heat exchanger," *Applied Thermal Engineering,* vol. 103, pp. 112-127, 2016/06/25/ 2016.
[12] S. Sakib and A. Al-Faruk, "Flow and Thermal Characteristics Analysis of Plate–Finned Tube and Annular–Finned Tube Heat Exchangers fo In–Line and Staggered Configurations," *Mechanics and Mechanical Engineering,* vol. 22, pp. 1407-1417, 01/01 2018.
[13] M. Zeeshan, S. Nath, and D. Bhanja, "Numerical study to predict optimal configuration of fin and tube compact heat exchanger with various tube shapes and spatial arrangements," *Energy Conversion and Management,* vol. 148, pp. 737-752, 2017/09/15/ 2017.
[14] S. Unger, E. Krepper, M. Beyer, and U. Hampel, "Numerical optimization of a finned tube bundle heat exchanger arrangement for passive spent fuel pool cooling to ambient air," *Nuclear Engineering and Design,* vol. 361, p. 110549, 2020/05/01/ 2020.
[15] S. Toolthaisong and N. Kasayapanand, "Effect of Attack Angles on Air Side Thermal and Pressure Drop of the Cross Flow Heat Exchangers with Staggered Tube Arrangement," *Energy Procedia,* vol. 34, pp. 417-429, 2013/01/01/ 2013.
[16] A. A. Gholami, M. A. Wahid, and H. A. Mohammed, "Heat transfer enhancement and pressure drop for fin-and-tube compact heat exchangers with wavy rectangular winglet-type vortex generators," *International Communications in Heat and Mass Transfer,* vol. 54, pp. 132-140, 2014/05/01/ 2014.

[17] S. Kumar Sarangi and D. Prasad Mishra, "Effect of tube shape on thermo-fluid performance of a winglet supported fin-and-tube heat exchanger having staggered tubes," *Materials Today: Proceedings,* 2020/10/12/ 2020.

[18] A. Adam, A. Oumer, A. Alias, M. Ishak, and M. M. Noor, "Investigation of thermal-hydraulic performance in flat tube heat exchangers at various tube inclination angles," *INTERNATIONAL JOURNAL OF AUTOMOTIVE AND MECHANICAL ENGINEERING,* vol. 14, pp. 4542-4560, 09/30 2017.

[19] A. Y. A. MOHAMMED, "EFFECT OF TUBE INCLINATION ANGLE ON THE THERMAL AND FLUID DYNAMIC PERFORMANCE OF FLAT TUBE HEAT EXCHANGER," Master of Enginnering (Mechanical), Faculty of Mechanical Enginnering, Universiti Malaysia Pahang, UMP Library, 2017.

[20] H. Kalantari, S. A. Ghoreishi-Madiseh, J. C. Kurnia, and A. P. Sasmito, "An analytical correlation for conjugate heat transfer in fin and tube heat exchangers," *International Journal of Thermal Sciences,* vol. 164, p. 106915, 2021/06/01/ 2021.

[21] J. Hoffmann-Vocke, J. Neale, and M. Walmsley, "The effect of fin-and-tube heat exchanger resistance on inlet flow maldistribution related pressure drop penalties," *17th Australasian Fluid Mechanics Conference 2010,* 01/01 2010.